Journal of Thermal Analysis, Vol. 30 (1985) 177–185

KINETICS AND MECHANISM OF PRECIPITATION PROCESSES IN Al–Ag ALLOYS

J. Kwarciak

INSTITUTE OF PHYSICS AND CHEMISTRY OF METALS, SILESIAN UNIVERSITY, 12, BANKOWA, 40-007 KATOWICE, POLAND

(Received June 5, 1984)

During the heating of a supersaturated solid solution, four peaks were observed in the DTA curve. Two exotherms were due to the precipitation of Guinier–Preston zones and an equilibrium phase. Endotherms accompanied dissolution of the zones and a stable precipitate.

The temperatures of the peaks, the thermal effects and the activation energy of precipitation appear to depend on the chemical compositions of the alloys.

Precipitation process in Al–Ag alloys

X-ray and microscopy data [1–3] on Al–Ag alloys lead to the conclusions that the structural changes may be described by the sequence: supersaturated $\alpha \rightarrow$ spherical Guinier–Preston (G. P.) zones $\rightarrow$ hexagonal intermediate Al_2Ag-type precipitate, $\gamma' \rightarrow$ stable Al_2Ag precipitate γ.

The G. P. zones are essentially solute-rich clusters, completely coherent with the matrix. Below 175° the G. P. zones are in the ordered η-state, which characterizes the cold age-hardening of the alloy. Above 220° the G. P. zones are in the ϵ-state (reversion of cold age-hardening), characterized by a disordered arrangement of atoms [4]. The precipitate grows as a faulted structure, but after long ageing times the faults are removed and the lattice becomes ordered. The transformation occurs by discontinuous precipitation involving a grain growth mechanism [5].

Calorimetric investigation indicates three transformations [6–8]. Two exothermic reactions accompany the precipitate of G. P. zones and the formation of a precipitate. The endotherm is due to the redissolution of the G. P. zones. The maximum value of the heat of precipitation increased from 2.9 to 16.8 J/g as the silver content in the alloy increased from 5 to 38 wt. %. The heat absorbed during redissolution also increased to 6.3 J/g with increasing Ag content.

DTA and calorimetry were used to investigate the precipitation processes in Al–Cu, Al–Cu–Mg–Mn [9–13], Al–Zn–Mg [14–16], Al–Mg–Si [17–18] and Al–Zn alloys [19, 20].

John Wiley & Sons, Limited, Chichester
Akadémiai Kiadó, Budapest

Kinetics of precipitation in Al–Ag alloys

The nucleation and growth of particles during precipitation determined by diffusion can be expressed by an approximate form of the equation [2]:

$$\alpha = 1 - \exp(-kt)^R \tag{1}$$

where R is a constant depending on the interface reaction, the particle size and the geometry, and t is time.

The change in size of the G. P. zones is due to the volume free energy. The normal growth of the zones is due to zone boundary energy.

This energy is reduced by zone growth, since the number of zones decreases as the zone volume increases.

Turnbull [21] has shown that the kinetics law for clustering in Al–Ag alloys is of the form

$$\alpha = 1 - \left(\frac{1}{1+bt}\right)^{\frac{1}{3}} \tag{2}$$

and is not a sigmoidal equation (1). b is a constant.

The isothermal rate law has previously been found empirically to be [4]:

$$R_1^4 - R_{1.0}^4 = \frac{k}{t - t_0} \tag{3}$$

R_1 and $R_{1.0}$ are the radii after ageing for times t and t_0.

The temperature-dependence of the reaction constant in the range 25–300° gave a single activation energy of $E = 94.5$ kJ/g atom for Al–Ag 20, 28 and 35 wt. % alloys.

Koster and Sperner [22] reported that the activation energy decreased linearly with the silver content in accordance with the equation: $E = 32.6 - 5.6x$ at. % silver. Hren and Thomas [23] found that the nucleation, growth and dissolution of the γ' precipitate in Al–Ag 20% alloy are completely reversible. Kinetic data obtained from the rates of dissolution of particles permit determination of the diffusion coefficient; the activation energy found is 157.5±16 kJ/mol.

Experimental

The investigations were performed with a Mettler Thermoanalyzer TA1. Samples of alloys were formed pure 99.995% Al and 99.99% Ag. Al–Ag 6, 10, 20, 30 and 40±0.2 wt. % alloys were prepared in a BCG-265 furnace. The samples were homogenized for 24 hours at 550°. Dissolution heat treatment for 3 hours at 550° was conducted in a vertical tube furnace with a flowing argon atmosphere. The ageing processes were investigated immediately after quenching in water, during linear heating, with DTA curve registration. The cylindrical samples, of about 2 g, were put in a macro-DTA crucible. A PtRh–Pt thermocouple was used.

Results and discussion

A typical DTA curve for Al–Ag alloy, heated immediately after quenching, is shown in Fig. 1. For the majority of the specimens, four peaks are observed, designated P_1, P_2, P_3 and P_4. They show the successive stages of the process. P_1 is an exotherm, usually commencing at about 50°, peaking at 110–120° and reaching the baseline at 150°. This peak is due to the precipitation of G. P. zones. Symmetric scattering about the incident beam in the X-ray picture obtained by the method of small angle scattering (SASX) confirms the presence of the G. P. zones [24] (Fig. 2a).

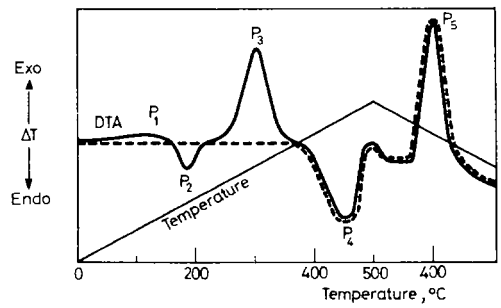

Fig. 1 DTA curve for Al–Ag 30 wt. %. Heating rate 8 deg/min

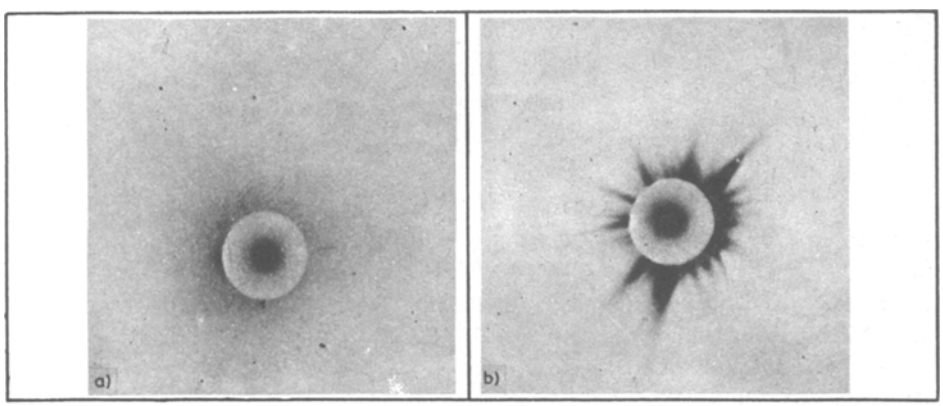

Fig. 2 SASX-ray picture of Al–Ag 30 wt. %; (a) for alloy heated for 3 hours in 120°, (b) for alloy heated up to 340°

The next evolution, P_2, involving absorption heat, extends over the range 150–200°. This endotherm is due to the partial redissolution of G. P. zones, or strictly speaking to the change of the η-state of the G. P. zones into the disordered ϵ-state. The exotherm P_3 extends over the range 220–300° and accompanies precipitation of both the intermediate and the stable precipitate. The streaks appearing on a spherical symmetric background on SASX confirm the presence of the γ-phase in the alloy

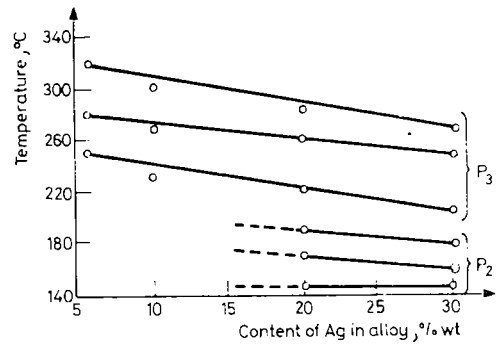

Fig. 3 Influence of the change in Ag content of Al—Ag alloys on the temperature ranges of peaks P_2 and P_3

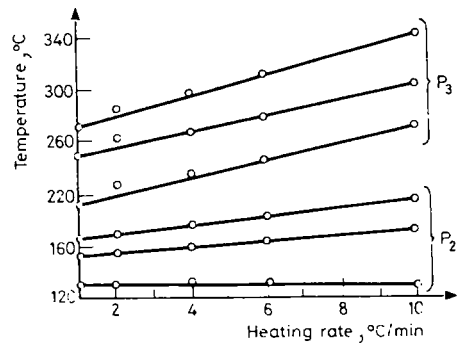

Fig. 4 Influence of the heating rate on the temperature ranges of peaks P_3 and P_4

(Fig. 2b). P_4 is an endotherm, starting when P_3 is finished. This peak is due to the dissolution of the precipitate. A fifth peak, exotherm P_5, appears during the cooling of samples from 500°. This peak accompanies the precipitation in Al—Ag alloys. During subsequent heating and cooling, peaks P_4 and P_5 appear repeatedly.

The positions, areas and shapes of these peaks were found to vary with variation of the silver content and the heating rate (Figs 3 and 4). The heats of reversion of the G. P. zones and precipitation of the ϵ-phase, designated ΔH_2 and ΔH_3, were calculated from the areas under peaks P_2 and P_3 by multiplying by the equivalent calories per unit area. The areas of peaks P_2 and P_3 were limited by a dashed line, obtained during repeated heating of the same sample of the alloy after cooling in the thermoanalyzer. The calibration coefficient, K, from the equation $\Delta H = KA$, where ΔH is the heat of the process and A is the area under the peak, was calculated over the range 100—600°.

Peak P_1 is hardly visible in the DTA curve and P_4 is unsymmetrical. Because of this, the thermal effects associated with precipitation of the G. P. zones (P_1) and dissolution of the precipitate (P_4) were not calculated.

Table 1 Influence of the silver content on the heats of dissolution of G. P. zones and precipitation in alloys

Silver content in Al–Ag alloy, wt. %	Heat of dissolution of G. P. zones, J/g	Heat of precipitation of γ-phase, J/g
6	–	3.36±0.42
10	–	5.88±0.63
20	1.05±0.21	9.66±0.63
30	4.18±0.42	14.70±0.84

Table 1 shows the influence of the silver contents the alloys on the heats of dissolution of the G. P. zones and precipitation.

The problem of deriving kinetics parameters from a DTA curve obtained under non-isothermal conditions has been faced by many authors. A complete review has been presented by Sestak, Satava and Wendlandt [25]. The calculation of kinetics parameters is often simplified and may be based on the assumption that the course of the reaction can be described by the differential equation

$$\frac{d\alpha}{dt} = k(T)f(\alpha) \tag{4}$$

where α is the degree of conversion, $d\alpha/dt$ is the rate of reaction, $k(T)$ is the temperature-dependent rate constant and $f(\alpha)$ is a function which represents the hypothetical model of the reaction mechanism.

In a number of reactions the rate constants $k(T)$ are satisfactorily described by the Arrhenius equation

$$k(T) = Z \exp\left(-\frac{E}{RT}\right) \tag{5}$$

Z is the frequency factor proportional to the number of successful collisions of the reacting molecules and E is the activation energy.

The function $f(\alpha)$ for a solid-state reaction can generally be considered to be as follows [26]:

$$f(\alpha) = \alpha^m (1-\alpha)^n [\ln (1-\alpha)]^p \tag{6}$$

where m, n and p are empirically obtained exponent factors, one of them always being zero.

We have examined the kinetics of formation of the precipitate on the basis of peak P_3 in the DTA curve.

The degree of conversion α during linear temperature rise has been determined via the DTA peaks at various heating rates. It has been assumed that the quotient of the growth of the area of the DTA peak to the total area of the peak is proportional to the degree of conversion. These α values are reported in Fig. 5 as a function of the specimen temperature.

The DTA peaks P_3 are characterized by a pronounced symmetry, and therefore the temperature of half-precipitation (transformed fraction $\alpha = 0.5$) coincides with the temperature of the peak.

Figure 6 shows how the experimental points linearly fit the logarithmic plot (Φ/T_m^2), where Φ is the rate of heating and T_m is the peak temperature, as a function of the reciprocal absolute peak temperature (Kissinger's method).

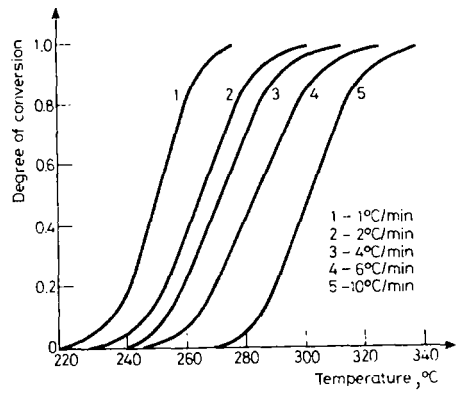

Fig. 5 The degree of conversion as a function of temperature (linear temperature rise at different rates)

The activation energy and pre-exponential factors found with Kissinger's method are shown in Table 2. The frequency factor is evaluated on the basis of the equation

$$Z = \frac{\frac{E\Phi}{RT^2}}{\exp\left(-\frac{E}{RT_m}\right)} \tag{7}$$

The kinetic treatment by Borchardt and Daniel's method may be adopted to all the types of kinetics in solids via the equation [27]:

$$k(T) = \frac{\frac{\Delta T}{A}}{\alpha^m (1-\alpha)^n [-\ln (1-\alpha)]^p} \tag{8}$$

where A is the area under the DTA peak.

Equation (8) can be used to determine the kinetics parameters of processes with a known empirical $f(\alpha)$ function. The best linear correlations have been obtained for

$$f(\alpha) = (1-\alpha)^{1.5}[-\ln (1-\alpha)]^{\frac{1}{3}} \tag{9}$$

These are shown in Fig. 7.

Calculations were made with a Mera-400 microcomputer. The activation energy and frequency factors are given in Table 2.

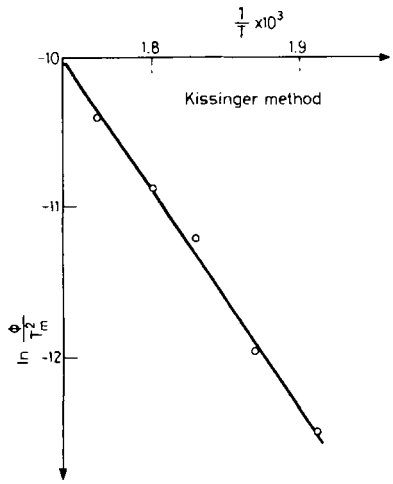

Fig. 6 Kissinger plots showing the dependence of peak temperature T_M on the heating rate Φ for the DTA curve of Al—Ag 30 wt. %

Table 2 Kinetic parameters obtained for Al—Ag alloys with Kissinger's and Borchardt—Daniel's methods

Silver content in Al—Ag alloys, wt. %	Kissinger's method		Borchardt—Daniel's method	
	E, J/mol	$\log Z$, sec^{-1}	E, J/mol	$\log Z$, sec^{-1}
6	136.5± 10.5	486.8± 3.3	174.3± 12	64.26± 3.3
10	128.9± 10.5	446.9± 3.3	156.7± 12	58.29± 3.3
20	117.6± 10.5	428.4± 3.3	151.2± 12	57.46± 3.3
30	111.3± 10.5	411.2± 3.3	140.7± 12	52.92± 3.3

The activation energy values obtained with Borchardt and Daniel's method are larger than those evaluated with Kissinger's method. A better linear correlation was obtained with the Borchardt and Daniel method, and thus these results seem more probable. With the increase in Ag content of the alloys the activation energy for precipitate formation decreases. This is an agreement with the calculations of Koster and Sperner [22] and Turnbull [21] for a low-temperature clustering process. However, it does not agree with the results of Baur and Gerold [4], who obtained a constant value of activation energy for Al—Ag 20, 28 and 35 wt. % alloys in the temperature range 25–300°.

The evaluated values of the frequency factor are in the range 10^{10}–10^{15} sec^{-1} in all cases, which is typical of solid-state reactions.

The values of m and p in Eq. (6) can be obtained when the value of R in Eq. (1) is about 1.5 [2].

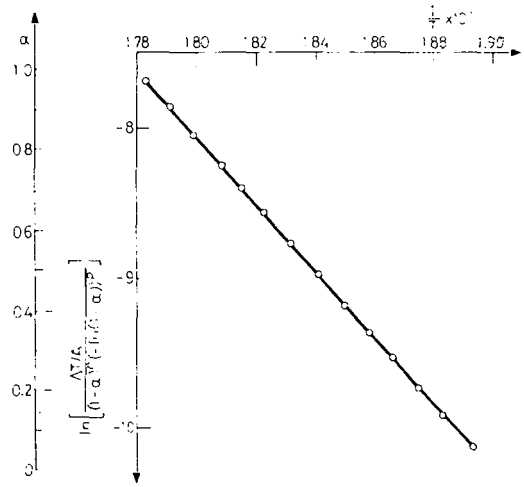

Fig. 7 Arrhenius plot of $\ln k$ vs. $1/T$ according to the Borchardt and Daniel method for Al–Ag 30 wt. %

If diffusion-limited growth begins from particles with an initial volume of more than about one-tenth of the final volume, R in Eq. (1) has a value between 1 and 1.5 [2].

In our case the equilibrium phase grows on G. P. zones which have not been dissolved. Thus, this is the process of growth of particles having small initial dimensions. We can draw the conclusion that the examined process agrees with the assumptions discussed above.

Conclusions

During heating of a supersaturated solid solution, four peaks, corresponding to the formation and dissolution of G. P. zones and precipitates, were observed in the DTA curve. It appears that the temperatures and the thermal effects of the successive changes depend on the chemical compositions of the alloys. The activation energy and the frequency factor of the formation of the stable γ-phase were established according to Kissinger's method and Borchardt–Daniel's modified method.

With the increase of the Ag content, the activation energy for precipitate formation decreases. The formula

$$f(\alpha) = (1-\alpha)^{1.5}[-\ln(1-\alpha)]^{\frac{1}{3}}$$

express the dependence of the transformed fraction during precipitation of the γ-phase.

According to this formula, it can be concluded that the process of particle growth in Al–Ag alloys is diffusion-controlled.

References

1 J. W. Martin, Precipitation Hardening, Pergamon Press, Oxford, 1968.
2 J. Christian, The Theory of Transformation in Metals and Alloys, Pergamon Press, Oxford, 1965.
3 H. K. Hardy and T. J. Heal, Report on Precipitation, Prog. in Met. Physics., Vol. 5, Pergamon Press, Oxford, 1954.
4 R. Baur and V. Gerold, Acta Met., 10 (1962) 637.
5 R. B. Nicholson and J. Nutting, Acta Met., 9 (1961) 332.
6 K. Hirano, Phys. Soc. Japan, 8 (1953) 603.
7 W. Koster and H. A. Schnell, Z. Metallk., 43 (1952) 454.
8 F. W. Jones and P. Leech, Nature, 147 (1941) 327.
9 G. Borelius and L. Strom, Arkiv. Mat. Astron. Physik, 21, 32A (1945).
10 N. Swindells and C. Sykes, Proc. Roy. Soc., A 168 (1938) 273.
11 T. Suzuki, Sci. Rep. Tohoku Univ., A 1 (1949) 183.
12 W. Fraenkel, Metallwirtschaft, 12 (1933) 583.
13 L. P. Luznikov and L. G. Berg, Zavodskaya Laboratorija, 14 (1948) 824.
14 K. Hirano and Y. Tagaki, J. Phys. Soc. Japan, 10 (1955) 187.
15 K. Asano and K. Hirano, Trans. Jap. Inst. of Metals, 9 (1968) 24, 149.
16 K. Hirano and K. Asano, Trans. Jap. Inst. of Metals, 11 (1970) 225.
17 J. Hajdu, L. Kertész, Cs. Lénárt and E. Nagy, Crystal Lattice Defects, 5 (1974) 177.
18 M. Farkas, M. Kovács-Treer and É. Závodi, J. Thermal Anal., 11 (1977) 241.
19 A. Zahra, Ch. Zahra and M. Laffitte, Z. Metallk., 70 (1979) 669.
20 P. Adler, G. Geschwind and R. Delasi, in Thermal Analysis, Vol. 2, Birkhäuser Verlag, Basel, 1972, p. 747.
21 D. Turnbull, M. S. Rosenbaum and H. N. Treafitis, Acta Met., 8 (1960) 277.
22 W. Koster and F. Sperner, Z. Metallk., 44 (1953) 217.
23 J. A. Hren and G. Thomas, Trans. Met. Soc. AIME, 227 (1963) 308.
24 A. Guinier and G. Fournet, Small Angle Scattering of X-rays, Wiley, New York, 1955.
25 J. Sestak, V. Satava and W. Wendlandt, Thermochim. Acta, 7 (1973) 333.
26 J. Sestak and G. Berggren, Thermochim. Acta 3 (1971) 1.
27 A. Lucci and M. Tammanini, Thermochim. Acta, 13 (1975) 147.

Zusammenfassung — Während des Aufheizens einer übersättigten festen Lösung wurden in der DTA-Kurve vier Peaks beobachtet. Zwei exotherme Effekte wurden der Ausscheidung von Guinier—Preston-Zonen und einer Gleichgewichtsphase zugeschrieben. Die Auflösung der Zonen und des stabilen Präzipitats gehen mit endothermen Effekten einher. Die Peaktemperaturen, die thermischen Effekte und die Aktivierungsenergie der Ausscheidung scheint von der chemischen Zusammensetzung der Legierungen abzuhängen.

Резюме — При нагревании пересыщенного твердого раствора на кривой ДТА проявлялись четыре пика. Два экзотермических пика обусловлены осаждением зон Гунье—Престона и образованием равновесной фазы. Эндотермические пики вызваны растворением таких зон и стабильного осадка. Температуры пиков, термические эффекты и энергия активации реакции осаждения зависят от химического состава сплавов.